Human Reproduction, Vol.31, No.4 pp. 854–865, 2016
Advanced Access publication on February 6, 2016 doi:10.1093/humrep/dew003

human reproduction

ORIGINAL ARTICLE ***Reproductive biology***

NMR-based metabonomics for understanding the influence of dormant female genital tuberculosis on metabolism of the human endometrium

E. Subramani[1], M. Jothiramajayam[2], M. Dutta[1], D. Chakravorty[1], M. Joshi[3], S. Srivastava[3], A. Mukherjee[2], C. Datta Ray[4], B.N. Chakravarty[5], and K. Chaudhury[1,*]

[1]School of Medical Science and Technology, Indian Institute of Technology Kharagpur, Kharagpur 721302, India [2]Cell Biology and Genetic Toxicology Laboratory, Centre of Advanced study, Department of Botany, University of Calcutta, Kolkata 700019, India [3]National Facility for High-field NMR, Tata Institute of Fundamental Research, Mumbai 400005, India [4]Department of Obstetrics and Gynaecology, Institute of Post-Graduate Medical Education and Research (IPGME&R) and SSKM Hospital, Kolkata 700020, India [5]Institute of Reproductive Medicine, Kolkata 700020, India

*Correspondence address. School of Medical Science and Technology, Indian Institute of Technology Kharagpur 721302, West Bengal, India. Tel: +91-3222-283572; Fax: +91-3222-282221; E-mail: koel@smst.iitkgp.ernet.in, koeliitkgp@gmail.com

Submitted on October 27, 2015; resubmitted on December 24, 2015; accepted on January 5, 2016

STUDY QUESTION: Does investigation of metabolic perturbations in endometrial tissue of women with dormant genital tuberculosis (GTB) during the window of implantation (WOI) assist in improving the understanding of endometrial receptivity?

SUMMARY ANSWER: In dormant GTB cases significant alterations in endometrial tissue metabolites occur, largely related to energy metabolism and amino acid biosynthesis in dormant GTB cases.

WHAT IS KNOWN ALREADY: As an intracellular pathogen, *Mycobacterium tuberculosis* strongly influences the metabolism of host cells causing metabolic dysregulation. It is also accepted that dormant GTB impairs the receptive status of the endometrium. Global metabolic profiling is useful for an understanding of disease progression and distinguishing between diseased and non-diseased groups.

STUDY DESIGN, SIZE, DURATION: Endometrial tissue samples were collected from patients reporting at the tertiary infertility care center during the period September 2011–March 2013. Women having tested positive for GTB were considered as the study group ($n = 24$). Normal healthy women undergoing sterilization ($n = 26$) and unexplained infertile women with repeated IVF failure ($n = 21$) volunteered to participate as controls.

PARTICIPANTS/MATERIALS, SETTING, METHODS: Endometrial tissue samples were collected 6–10 days after confirmation of ovulation. PCR and BACTEC-460 culture were used for diagnosing GTB. Proton nuclear magnetic resonance (1H NMR) spectra of tissue were recorded using a 700 MHz Bruker Avance AV III spectrometer. Following phase and baseline correction of all NMR spectra by Bruker Topspin 2.1 software, spectral peak alignment of the data was performed. Multivariate analysis was applied to all spectra and individual metabolites identified and multiple correlation analysis was performed.

MAIN RESULTS AND THE ROLE OF CHANCE: Leucine, isoleucine, acetate, lactate, glutamate, glutamine, methionine, lysine, creatine, glycogen, glycine, proline and choline were found to be significantly increased ($P < 0.05$) in endometrial tissue of women with dormant GTB compared with unexplained infertile women with repeated implantation failure. Valine, citrate, succinate and aspartate were also observed to be significantly up-regulated ($P < 0.01$). Furthermore, a significant decrease in glucose ($P < 0.05$), threonine ($P < 0.05$), tyrosine ($P < 0.01$) and phenylalanine ($P < 0.0001$) was observed in women with dormant GTB. Pearson's correlation analysis between the expression of various endometrial receptivity markers and metabolites showed a significant negative correlation (-0.236 to -0.545, $P < 0.05$). Also, the metabolites were positively correlated with endometrial receptivity markers (0.207 to 0.618, $P < 0.05$).

LIMITATIONS, REASONS FOR CAUTION: It is often difficult to diagnose dormant GTB because it tends to exist without any clinical signs or symptoms. In addition, the diagnosis of GTB by culture remains a challenge due to low detection rates and its paucibacillary nature. Testing for

prostate-specific antigen or the Y chromosome in order to account for the possible influences of recent exposure to semen on endometrial metabolism would be important.

WIDER IMPLICATIONS OF THE FINDINGS: The metabolic changes associated with the dormant tubercle infection are of potential relevance to clinicians for the treatment of dormant GTB-related infertility.

STUDY FUNDING/COMPETING INTEREST(S): Government of India, Indian Council of Medical Research. There are no conflicts of interest.

Key words: proton nuclear magnetic resonance / metabonomics / endometrial receptivity / dormant genital tuberculosis / endometrial tissue

Introduction

Tuberculosis (TB), caused by the bacterial pathogen *Mycobacterium tuberculosis*, generally results in a chronic or latent infection and has been correctly recognized as a global emergency (Gatongi *et al.*, 2005). TB can spread from its origin of pulmonary or abdominal infection through the hematogenous route and cause extra-pulmonary TB (Rozati *et al.*, 2006). About 9% of all extra-pulmonary TB cases are genital TB (GTB), which causes irreversible damage to the genital organs of younger women of reproductive age (Thangappah *et al.*, 2011; Sankar *et al.*, 2013). Infertility is the primary symptom of GTB and is also associated with various other complications (Sankar *et al.*, 2013). In developed countries, the prevalence of GTB is estimated to be 1%, whereas, in India it is reported to be as high as 18–19% among infertile women aged 20–40 years (Das *et al.*, 2008). A case study by Kocher *et al.* (2011) reported that GTB has been diagnosed in the Western European countries which reflects increasing occurrence of GTB in these regions. Another challenging problem often faced by the clinician is the diagnosis and management of dormant GTB. Dormant GTB in women is defined as the condition when dormant but viable tubercular bacilli reside in the genital tract for a considerable period of time without any signs or symptoms, but are capable of reactivating themselves to cause the disease (Malik, 2003). Due to its asymptomatic nature, the exact incidence and prevalence of dormant GTB is largely unknown.

The window of implantation (WOI) refers to the 6–10 day period post ovulation, when the endometrium is receptive to the embryo at the blastocyst stage (Wilcox *et al.*, 1999; Martin *et al.*, 2002; Haouzi *et al.*, 2009). Advances in assisted reproductive technologies have contributed significantly toward the selection of high quality embryos during IVF; however, the receptive status of the endometrium remains the limiting factor for successful conception. In fact, reduced endometrial receptivity is believed to be one of the major causes of repeated implantation failure (Margalioth *et al.*, 2006; Ghosh *et al.*, 2013). In our earlier study, we have reported that dormant GTB is associated with subendometrial blood flow impairment and reduced endometrial thickness (Dam *et al.*, 2006). Hence, understanding the influence of dormant Mycobacterial bacilli on the endometrium at a metabolic level during the WOI seems clinically relevant.

Systems biology techniques including metabonomics are being increasingly used in understanding disease pathophysiology and in the development of reliable diagnostic biomarkers (Zhao *et al.*, 2014; Bujak *et al.*, 2014). Proton nuclear magnetic resonance spectroscopy (1H NMR) is established as one of the powerful tools for the analysis of low molecular weight metabolites in biofluids and tissues (Kostara *et al.*, 2014). Metabolomics deals with normal endogenous metabolism, whereas metabonomics is the study of perturbations in metabolism caused by external stimuli. However, the terms metabolomics and metabonomics are often used interchangeably. Multivariate statistical models such as principal component analysis (PCA), partial least squares discriminant analysis (PLS-DA), and orthogonal partial least squares discriminant analyses (OPLS-DA) are used to detect significant results.

NMR-based metabolomics studies on murine TB models (Shin *et al.*, 2011; Somashekar *et al.*, 2011, 2012) and lung TB patients (Weiner *et al.*, 2012; Zhou *et al.*, 2013; Frediani *et al.*, 2014) have shown remarkable changes in the metabolite profiling during infection. It is also reported that tubercle bacilli influence metabolism of the host cells, thus altering the metabolites in biofluids and tissues (Zhou *et al.*, 2013). In view of the fact that tubercle bacilli act as an intracellular pathogen, identification of the metabolic derangements during mycobacterial infection is likely to help in understanding the underlying mechanism of host-pathogen interaction (Somashekar *et al.*, 2012). No metabolomic profiles and outcomes of women with dormant GTB infection have been reported so far. The present study investigates 1H NMR metabolic profiling of endometrial tissue infected with dormant/latent tubercle infection as compared with proven fertile women and unexplained infertile women with repeated IVF failure.

Materials and Methods

Subject selection and sample collection

This study was conducted with the prior approval of the human ethics committee of the Institute of Reproductive Medicine (IRM), Kolkata and Indian Institute of Technology, Kharagpur. Written informed consent was obtained from all couples participating in the study. The inclusion criteria ensured that only women <40 years with regular menstrual cycles (25–32 days), who were euthyroid with normal baseline FSH and prolactin levels with no identifiable cause of infertility (unexplained infertility) were included. Endometrial tissue samples were obtained by dilation and curettage from women with repeated IVF failure (>3 attempts of embryo transfer) and diagnosed for GTB by PCR and BACTEC-460 culture. Women found to be positive for GTB were included as one study group ($n = 24$). Of these, five women had a history of pulmonary TB. Two groups were included as controls: (i) proven fertile healthy women (given birth in the last 2–3 years) undergoing voluntary sterilization (Control 1; $n = 26$) and (ii) unexplained infertile women with repeated IVF failure (Control 2; $n = 21$). Women who had their last delivery during the 2–3 preceding years and had used only male barrier methods (not any other form of contraception) were included in the study as proven fertile women. The cases and controls were comparable in terms of age, BMI, hormone levels, ethnicity, geographical residence, sexual activity and sex partners. All controls tested negative for GTB by both BACTEC-460 and PCR. Daily ovarian ultrasonography and a urinary LH assay were performed for ovulation confirmation (Banerjee *et al.*, 2013). Endometrial tissue samples were collected from all groups 6–10 days post

ovulation. Endometrial histology was performed to confirm the biopsied samples correspond to mid-secretory endometrium.

Women with a history of chocolate cyst, fibroids, mild to severe endometriosis, polycystic ovary syndrome, *Chlamydia trachomatis* or other infections (*Neisseria gonorrhoeae, Trichomonas vaginalis, Treponema pallidum, Mycoplasma genitalium, Mycoplasma hominis, Ureaplasma urealyticum, Gardnerella vaginalis and Candida albicans*), bacterial vaginosis and viral infections (human immunodeficiency virus, herpes simplex virus type 2, human papillomavirus and hepatitis-B) and any pelvic pathology including pelvic inflammatory disease and adhesions were excluded. Cervical swabs were collected from all women and subjected to PCR testing and culture for *Chlamydia trachomatis* species. Women with any uterine abnormalities were excluded based on the Grading of Recommendations, Assessment, Development and Evaluation score by Galliano et al. (2015).

Metabolite extraction

Endometrial tissue samples were snap-frozen and stored at −80°C until extraction of metabolites using perchloric acid, as described elsewhere (Beckonert *et al.*, 2007). Briefly, the frozen tissue (100 mg wet weight) was homogenized in 6% ice-cold perchloric acid and kept in ice for 10 min. Following centrifugation at 12000 ×g for 10 min, the supernatant was neutralized to pH 7.4 with 2M potassium carbonate (K_2CO_3) and left for 30 min in ice to precipitate the potassium perchlorate salts. The supernatant was freeze-dried and stored at −80°C until analysis.

1H NMR spectrometry

One-dimensional 1H NMR spectra of tissue samples were acquired by applying Carr-Purcell-Meiboom-Gill (CPMG) pulse sequence to suppress signals of water and macromolecules. The detailed experimental procedure is described elsewhere (Dutta *et al.*, 2012; Jana *et al.*, 2013; Banerjee *et al.*, 2014). Briefly, polar tissue extracts were resuspended in 600 µl of D_2O containing 1 mM sodium salt of 3-(trimethylsilyl) propionic-2, 2, 3, 3, d4 acid (TSP), a chemical shift reference. The mixture was then vortexed, centrifuged and loaded into 5 mm NMR tubes. NMR spectra were recorded on a 700 MHz Bruker Avance AV III spectrometer at 298 K with 256 transients, spectral width of 14 005.6 Hz, 16K data points, relaxation delay 4.0 s, and an acquisition time of 0.58 s.

Spectra pre-processing

Acquired spectra were manually phase and baseline corrected, and chemical shifts referenced to TSP ($\delta = 0.0$ ppm) in MestReNova version 7.1.0 (Mestrelab Research, Santiago de Compostela, Spain). Spectral region of δ 0.5–4.4 (excluding residual water signal: δ 4.5–5.10 ppm) was subjected to multivariate analysis. Univariate analysis was performed separately for the region δ 5.10–9.0 since this region represents poor signal to noise ratio. Recursive segment-wise peak alignment (RSPA) was applied to the spectral region of δ 0.5–4.4 ppm for minimizing chemical shift variations using the R/Bioconductor package mQTL.NMR (Hedjazi *et al.*, 2015). Spectra were normalized to a constant sum to limit the effect of concentration differences between the samples. Unit variance scaling was applied to the data matrix for giving equal weightage to all the variables (SIMCA 13.0.2, Umetrics, Sweden).

Multivariate analysis and data validation

An unsupervised model, PCA was performed to determine the intrinsic clustering and distribution of samples between dormant GTB and controls. Supervised classification models including PLS-DA and OPLS-DA were applied to visualize class separation using SIMCA 13.0.2 (Umetrics, Sweden). OPLS-DA maximizes class segregation by removing variability irrelevant to class separation and builds a model detecting potential metabolites involved in discriminating dormant GTB and controls. Significant regions were identified based on S-plot and variable-importance in projection (VIP). The threshold of correlation coefficient (r) and VIP was set to $|r| \geq 0.6$ and VIP ≥ 1, respectively.

A permutation test with 200 iterations was carried out to validate the quality of the PLS-DA model. The robustness and validation of the OPLS-DA model against overfitting was determined by the following parameters: goodness of fit (R2), goodness of prediction (Q2) and analysis of variance testing of cross-validated predictive residuals (CV-ANOVA score). Receiver operating characteristic (ROC) curve analysis was also performed to validate the robustness and predictive performance of the constructed models in discriminating groups.

Univariate analysis

Peaks were assigned based on the human metabolome database (HMDB), literature (Mazzei *et al.*, 2010) and 2D NMR experiments [COSY (correlation spectroscopy) and TOCSY (total correlation spectroscopy)]. The statistically significant variables extracted were subjected to spectral integration using MestReNova version 7.1.0 (Mestrelab Research, Santiago de Compostela, Spain). Statistical comparison between the mean integral values of corresponding metabolites of dormant GTB and controls was performed using Student's *t*-test or Mann–Whitney test (GraphPad Prism version 5.00 for Windows, GraphPad Software, San Diego, CA, USA), as applicable. $P < 0.05$ was considered to be statistically significant. Multiple Pearson's correlation analysis was determined and represented as heatmaps using R statistical packages version 3.2.2 (R Foundation for Statistical Computing, Vienna, Austria; http://www.R-project.org/). Concentration of metabolites (i.e. integral values) was subjected to pathway analysis. Metabolite relationships were derived from metabolomics pathway analysis (MetPA, http://metpa.metabolomics.ca/MetPA/faces/Home.jsp; Xia and Wishart, 2010).

Results

Demographic characteristics of the participants

The demographic characteristics of women with dormant GTB and controls are summarized in Table I. Age, BMI, serum estrogen and progesterone levels, ethnicity, geographic region of residence, sexual activity and sex partners were found to be comparable between the groups. Endometrial histology confirmed that the biopsied samples correspond to the mid-secretory phase of the endometrium (Fig. 1).

Chemometric discrimination of dormant GTB and controls

Multivariate analysis was used to identify the metabolites associated with mycobacterial infection in the endometrium. For an unbiased reduction of the complexity of data sets, the unsupervised statistical approach PCA was applied to NMR spectra of the groups. PCA identified the general patterns and outliers from the scatter score plot of principal component 1 (PC1) versus PC2 and visualized the inherent clustering between dormant GTB women and controls. The PCA scores plot has shown a clear separation between the groups (Supplementary Fig. S1; R2X = 72.2%, Q2 = 0.51). The supervised classification models PLS-DA and OPLS-DA were generated to improve the class separation between dormant GTB and controls. The improved separation of dormant GTB and control groups in PLS-DA models was achieved by utilizing class membership of the observation (Fig. 2A; R2X = 52.9%, R2Y = 0.974,

Table I Clinical characteristics of women with dormant genital tuberculosis (GTB) and controls.

Parameters	Dormant GTB women	Proven fertile women (Control 1)	Unexplained infertile women with >3 IVF failure (Control 2)
Age (years)	34.4 ± 2.7	33.9 ± 2.3	32.8 ± 3.9
BMI (kg/m^2)	24.1 ± 2.3	24.8 ± 1.96	23.8 ± 1.8
Serum estrogen level (pg/ml)	240.12 ± 37.22	228.40 ± 29.66	235.65 ± 45.61
Serum progesterone level (ng/ml)	19.73 ± 2.8	20.94 ± 3.81	21.85 ± 5.48
Ethnicity	South Asian	South Asian	South Asian
Geographical residence	Eastern and North-east, India Nepal and Bangladesh	Eastern and North-east, India Nepal and Bangladesh	Eastern and North-east, India Nepal and Bangladesh
Sexual activity			
Frequency of sexual intercourse	3–5 times a week	2–3 times a week	3–5 times a week
Sex partners	Male (Monogamous)	Male (Monogamous)	Male (Monogamous)
Parity (for control 1)	–	2–3	–
Time since last delivery (for control 1)	–	2–3 years	–

Data are represented as mean ± SD. All groups were found to be comparable ($P > 0.05$); Student's *t*-test comparing dormant GTB cases with controls.

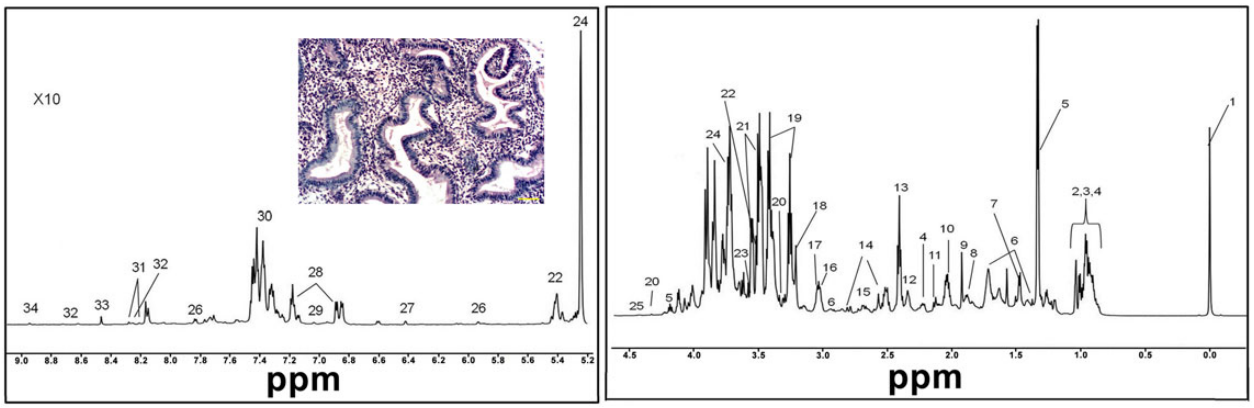

Figure 1 A typical 700 MHz 1H NMR spectrum (δ 9.0 − 0.0 ppm) of endometrial tissue obtained from a woman with dormant genital tuberculosis (GTB) with spectral assignment of metabolites. Numbers indicate the following metabolites: 1. 3-(trimethylsilyl) propionic-2,2,3,3,d4 acid (TSP), 2. Isoleucine, 3. Leucine, 4. Valine, 5. Lactate, 6. Lysine, 7. Alanine, 8. Arginine, 9. Acetate, 10. Glutamine, 11. Methionine, 12. Succinate, 13. Glutamate, 14. Citrate, 15. Aspartate, 16. Creatine, 17. Ornithine, 18. Choline, 19. Taurine, 20. Proline, 21. Myoinositol, 22. Glycogen, 23. Glycine, 24. Glucose, 25. Threonine, 26. Uracil, 27. Fumarate, 28. Tyrosine, 29. Histidine, 30. Phenylalanine, 31. Inosine, 32. Adenosine monophosphate (AMP), 33. Formate, 34. Nicotinamide. A representative image of endometrial histology of biopsied samples confirms the mid-secretory phase of the endometrium (inner panel), scale-50 μm.

and Q2 = 0.934). OPLS-DA model, an extension of PLS-DA, was further applied to remove the variables not related to the class separation for easy interpretation. This optimized classification between dormant GTB and control groups (Fig. 2C a,c,d). We also found the OPLS-DA model to fit well with the training data set and could predict the classes better than chance with higher R2 and Q2 values [Dormant GTB versus Control 1 (R2X = 50.3%, R2Y = 0.988 and Q2 = 0.971); Dormant GTB versus Control 2 (R2X = 38.7%, R2Y = 0.982 and Q2 = 0.957); Control 1 versus Control 2 (R2X = 47%, R2Y = 0.991 and Q2 = 0.967)]. R2 and Q2 are important parameters for assessing the variance and predictive ability of the model, respectively. High R2 and Q2 values indicate that the model has a good fit and can satisfactorily predict dormant GTB. R2X indicates the total amount of variation in X; R2Y indicates the total amount of variation in Y; and Q2 indicates the total amount of predictive variability in Y.

Supervised models, though capable of providing good discrimination, have a tendency to overfit the data. Therefore, the model was rigorously validated for good predictability and robustness of the model with regard to sample collection, data acquisition and processing, and inter-individual variations. A permutation test was used to validate whether the PLS-DA model has better predictive ability than 200 different permuted models. This validation method demonstrated that the original model has better predictive capability than the 200 Y-permutated models. This was demonstrated by the regression line of Q2 with intercept at −0.318 and R2 regression line intercept at 0.404, with all permuted R2 and Q2 values lower than the original value obtained from

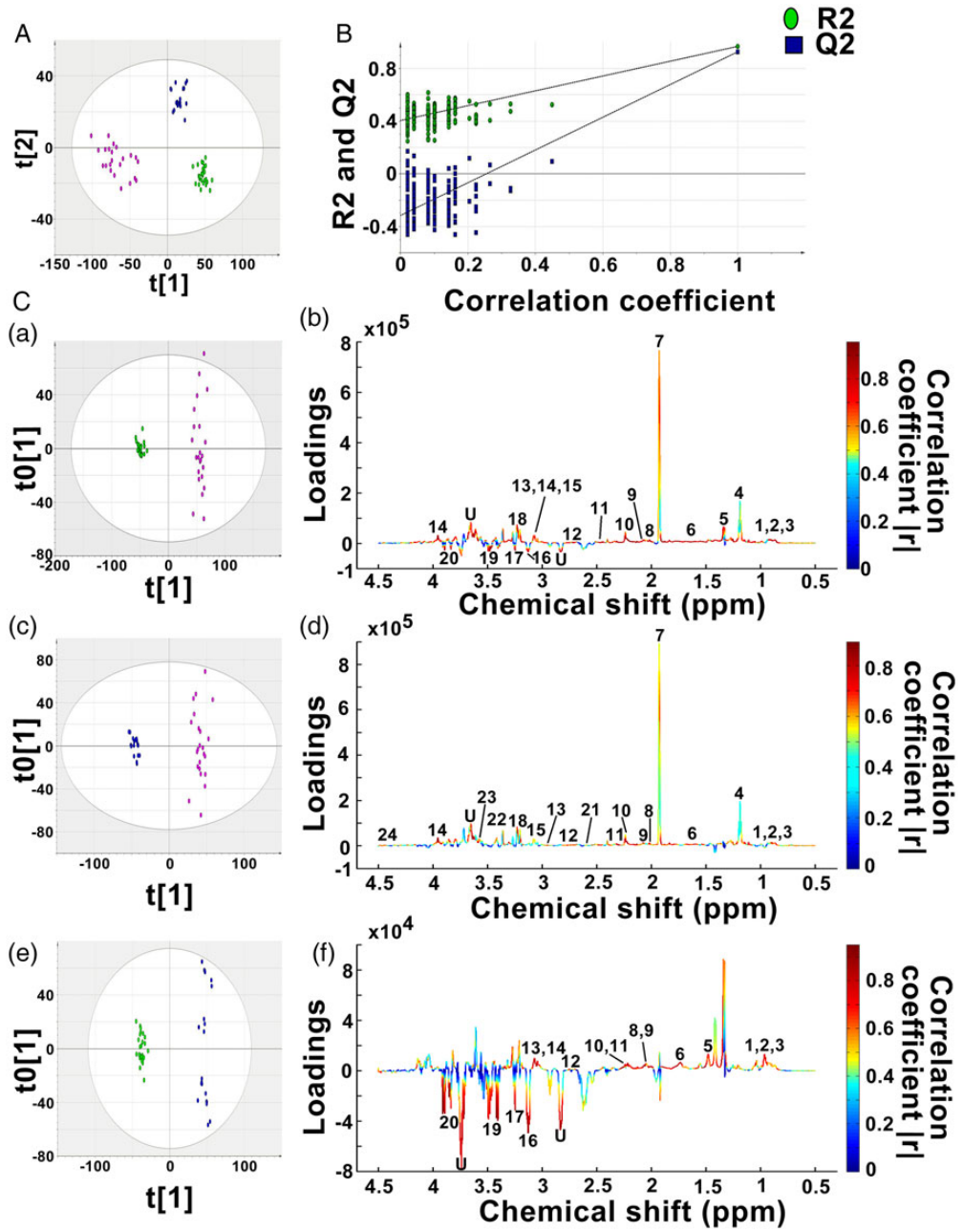

Figure 2 PLS-DA scatter plot, permutation tests and OPLS-DA coefficient loading plots as colormaps. (**A**) Two-dimensional scatter plot of PLS-DA shows discrimination of dormant GTB women (●) and controls (proven fertile women (●) and unexplained infertile cases with repeated IVF failure (●)). (**B**) Permutation test shows statistical validation of the PLS-DA model ($n = 200$). The regression line of Q2 (goodness of prediction) with intercept at −0.318 and R2 (goodness of fit) regression line intercept at 0.404 indicate that our model has higher R2 (goodness of fit) and Q2 (goodness of prediction) values in the validation test than the permutated models generated. (**C**) OPLS-DA score (left) and loading plot (right) for 1H NMR endometrial tissue spectra of (a) dormant GTB cases ($n = 24$) versus proven fertile women (control 1; $n = 26$), (b) dormant GTB cases ($n = 24$) versus unexplained infertile women with repeated IVF failure (control 2; $n = 21$), (c) control 1 ($n = 26$) versus control 2 ($n = 21$). Coefficient loading plots corresponding to OPLS-DA model are represented as color map (MATLAB R2009a, The MathWorks, Inc., USA). The color bar represents modulus of correlation for the variables/metabolites responsible for discriminating the groups (cut-off at $|r| > 0.6$; significance at $P < 0.05$). Positive and negative loadings show increased and decreased metabolites. Altered metabolites are indicated: 1. Isoleucine, 2. Leucine, 3. Valine, 4. Lactate, 5. Alanine, 6. Lysine, 7. Acetate, 8. Glutamine, 9. Methionine, 10. Succinate, 11. Glutamate, 12. Aspartate, 13. Creatine, 14. Ornithine, 15. Choline, 16. Arginine, 17. Taurine, 18. Proline, 19. Myoinositol, 20. Glucose, 21. Citrate, 22. Glycogen, 23. Glycine, 24. Threonine, U-unknown.

the model (Fig. 2B). Cross-validation of the OPLS-DA model with a CV-ANOVA score showed highly significant differences between the groups [Dormant GTB versus Control 1 ($P = 3.43939 \times 10^{-33}$); Dormant GTB versus Control 2 ($P = 3.63395 \times 10^{-26}$); Control 1 versus Control 2 ($P = 6.0387 \times 10^{-28}$)]. The CV-ANOVA score confirms that our model is statistically valid and more efficient than the permutated models in predicting the classes. Further, ROC analysis of the OPLS-DA model (area under ROC = 0.99) indicates better predictability and accuracy of the model.

Next, the validated OPLS-DA model was used for variable/metabolites extraction. Based on the S-plot and VIP plot, significant differences in concentration of the metabolites between the groups (dormant GTB versus control 1; dormant GTB versus control 2; control 1 versus control 2) were identified. The S-plot visualizes a correlation coefficient of the metabolites, which indicates the significantly dysregulated metabolites (Fig. 2C b,d,f). The VIP score also contributes toward the identification of the important variable/metabolites in discrimination of the groups (Supplementary Fig. S2A–C). The variables contributing toward class separation of disease and control groups were selected by setting the threshold of the correlation coefficient $> \pm 0.60$ (Fig. 2C) and VIP ≥ 1 (Supplementary Fig. S2A–C).

Metabolite profiles of endometrial tissue in dormant GTB and controls

A typical 1H CPMG-NMR spectrum of endometrial tissue obtained from a woman with dormant GTB is shown in Fig. 1. Thirty-four metabolites could be identified and assigned based on the literature and 2D NMR experiments (COSY and TOCSY).

Metabolite profiling associated with tubercle infection in the endometrium was obtained based on the significant regions identified in the S-plot and VIP scores and the integral values of these metabolites subjected to univariate analysis. Succinate, acetate, lactate, lysine, glutamine, glutamate, proline, valine, alanine, isoleucine, leucine, aspartate, methionine, choline, creatine and ornithine were significantly higher in endometrial tissue of women with dormant GTB as compared with proven fertile women (Table II). A significant decrease in taurine, myoinositol, glucose and arginine was observed in dormant GTB women compared with control 1 (Table II). A significant increase in valine, leucine, isoleucine, acetate, lactate, glutamate, glutamine, citrate, succinate, methionine, lysine, creatine, aspartate, glycogen, glycine, proline and choline and decrease in glucose, threonine, tyrosine and phenylalanine were observed in women with dormant GTB as compared with unexplained infertile women with repeated implantation failure (Table II). We observed increased levels of lysine, alanine, valine, leucine, isoleucine, glutamine, glutamate, aspartate, methionine, creatine, ornithine, tyrosine and phenylalanine and decreased levels of arginine, taurine, myoinositol and glucose in unexplained infertile women with repeated implantation failure as compared with proven fertile women (Table II).

Association between endometrial receptivity markers and blood flow parameters with the altered metabolites

Here, we also explore the possible association of the altered endometrial tissue metabolites with our earlier findings reporting dysregulated protein expression of various endometrial receptivity markers and endometrial blood flow parameters in women with dormant GTB (Subramani *et al.*, 2016). A significant negative correlation (-0.236 to -0.545, $P < 0.05$) was observed between the expression of various endometrial receptivity markers and acetate, aspartate, choline, creatine, glutamate, glutamine, leucine, methionine, proline, succinate, valine, lysine (except MECA79), isoleucine (except MECA79), ornithine (except MECA79) and glycogen [except MECA79 and vascular endothelial growth factor (VEGF)]. In addition, a negative correlation was observed for citrate and leukemia inhibitory factor (LIF), integrin β3 and MECA79, lactate with integrin β3, MECA79 and VEGF, and alanine with LIF, E-cadherin, integrin αv and mucin 1. In contrast, glucose, myoinositol and taurine were found to positively correlate with endometrial receptivity markers (0.207 to 0.618, $P < 0.05$; Fig. 3). Threonine with LIF, E-cadherin, integrin αv and integrin β3, glycine with LIF, E-cadherin and integrin αv and arginine with LIF, e-cadherin, integrin αv, Mucin 1 and MECA79 also showed a positive correlation (0.207 to 0.618, $P < 0.05$; Fig. 3). Furthermore, a significant negative correlation of alanine, aspartate, citrate, glutamine, leucine, lysine, methionine and succinate with end diastolic volume (EDV) and glucose with vascularization index (VI) was observed. Acetate, choline, glutamine, lysine, methionine, proline, succinate and valine with VI, glutamine with pulsatility index (PI), glutamate, isoleucine and lysine with resistance index (RI), glucose, myoinositol and taurine with EDV and aspartate, isoleucine, leucine, lysine, methionine and valine with systemic diastolic (S/D) ratio were found to be positively correlated (Fig. 3).

Metabolomic pathway analysis

Metabolomic pathway analysis (MetPA) was used to identify altered pathways involved in each group. Significantly altered metabolites in dormant GTB and unexplained infertile cases featured in 43 (Supplementary Table SI) and 38 pathways (Supplementary Table SII), respectively. Since these multiple pathways are analyzed at the same time in MetPA, *P*-values obtained from metabolite set enrichment analysis (Raw p) were subjected to tests at various levels. These tests include Holm–Bonferroni method (Holm p), false discovery rate adjustment (FDR p value) and pathway topology analysis based impact score. Following multi-step analysis using MetPA, metabolic pathways including the tricarboxylic acid (TCA) cycle, glycine, serine and threonine metabolism, aminoacyl-tRNA biosynthesis, phenylalanine metabolism and alanine, aspartate and glutamate metabolism were found to be significantly altered in dormant GTB (Supplementary Fig. S3A). Similarly, taurine and hypotaurine metabolism, arginine and proline metabolism, aminoacyl-tRNA biosynthesis, pyruvate metabolism, alanine, aspartate and glutamate metabolism were found to be associated with unexplained infertile cases (Supplementary Fig. S3B).

Discussion

Metabolic changes in the endometrium of dormant GTB women during the WOI

The present study, for the first time, attempts to investigate the metabolic milieu of the endometrium owing to the presence of dormant *Mycobacterium* bacilli infection. A total of 20 metabolites were found to be dysregulated in endometrial tissue of dormant GTB women compared with control 1 (proven fertile women) (Table II). Association of these metabolites with GTB seems likely. It was, nevertheless, critical to include an additional group of women with recurrent implantation failure and no other apparent cause of infertility (control 2) so that we

Table II Fold change of significant metabolites discriminating dormant GTB women and controls (unexplained infertile women with IVF failure and proven fertile women).

Metabolites	ppm	Fold change		
		Dormant GTB versus proven fertile women	Dormant GTB versus unexplained infertile women with IVF failure	Unexplained infertile women with IVF failure versus proven fertile women
Acetate (s)	1.91	13.56***	1.66*	–
Lactate (d)	1.32	1.56*	1.69*	–
Citrate (d)	2.56	–	2.28**	–
Succinate (s)	2.39	4.84**	3.78**	–
Aspartate (dd)	2.66	4.53***	1.83**	2.47***
Glycogen (m)	3.60	–	3.09*	–
Glucose (d)	5.2	0.245***	0.50*	0.49*
Choline (s)	3.19	2.94**	2.2*	–
Creatine (s)	3.02	2.46***	1.65*	1.44*
Ornithine (m)	3.04	3.46***	–	3.83**
Lysine (m)	1.71	2.13***	3.2*	1.46*
Valine (d)	1.02	3.68***	1.87**	1.97***
Leucine (t)	0.94	2.67***	1.62*	1.64**
Isoleucine (d)	0.99	2.78***	1.92*	1.45*
Glycine (s)	3.54	–	2.51*	–
Alanine (d)	1.46	2.89***	–	2.34**
Glutamate (m)	2.12	2.28**	1.71*	1.33*
Glutamine (m)	2.44	2.68***	1.73*	1.549*
Methionine (m)	2.15	3.39***	1.95*	1.74*
Proline (m)	3.33	3.25**	1.85*	–
Threonine (m)	4.24	–	0.19**	–
Tyrosine (m)	6.87	–	0.69*	1.362*
Phenylalanine (m)	7.36	–	0.081***	10.77***
Arginine (m)	1.90	0.59*	–	0.624*
Taurine (t)	3.25	0.435**	–	0.40***
Myoinositol (dd)	3.52	0.34***	–	0.323***

*$P < 0.05$; **$P < 0.01$; ***$P < 0.0001$; – Non-significant; Student's *t*-test or Mann–Whitney *U*-test, as applicable.
Multiplicities: s-singlet, d-doublet, t-triplet, m-multiplet, dd-doublet of doublets.

could clearly identify metabolic changes attributable to dormant GTB *per se*. A total of 21 metabolites were found to be significantly dysregulated on comparing dormant GTB with control 2.

Of the 20 significantly dysregulated metabolites (dormant GTB versus control 1), we found 15 altered metabolites to be common with the dormant GTB versus control 2 group (Table II). It is, therefore, logical to presume that the remaining five metabolites of dormant GTB versus control 1 group (taurine, myoinositol, arginine, ornithine and alanine) are due to the influence of unidentified endometrial factors in dormant GTB women. This assumption is further supported by our third set of comparative analyses between unexplained infertile women with repeated IVF failure and proven fertile controls (control 1 versus control 2). Once again, the same set of five metabolites observed earlier in the dormant GTB versus control 1 group were found to be present (Table II).

The endometrial metabolites associated with the dormant GTB condition could be largely related to the TCA cycle, glycine, serine and threonine metabolism, aminoacyl-tRNA biosynthesis, phenylalanine metabolism, and alanine, aspartate and glutamate metabolism with corresponding changes in energy metabolism and protein biosynthesis (Fig. 4; Supplementary Fig. 3A). Our findings are in good agreement with various NMR-based metabolomic reports on active lung TB of both humans and animals where alterations in the intermediates of the TCA acid cycle, glycolysis, oxidative phosphorylation and amino acid biosynthesis are observed (Shin *et al.*, 2011; Somashekar *et al.*, 2011, 2012; Weiner *et al.*, 2012; Zhou *et al.*, 2013; Frediani *et al.*, 2014).

Increase in glucose and energy metabolism

The metabolic profiles of endometrial tissue from women with dormant GTB showed enhanced glucose consumption and accumulation of lactate. These findings are in agreement with earlier reports which suggest that tubercle bacilli cause oxygen tension in the host and trigger the glycolytic pathway, which, in turn, increases glucose consumption and concurrent lactate production (Chen *et al.*, 2013). Accumulated

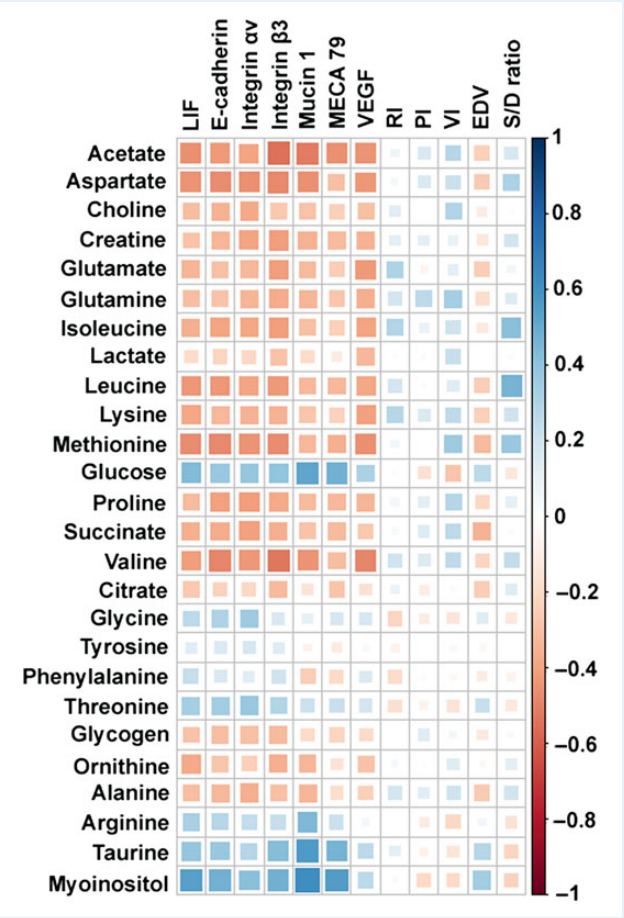

Figure 3 A correlation heatmap using Pearson's correlation. The heatmap represents the statistical association of endometrial metabolites with receptivity markers and blood flow parameters in dormant GTB women ($n = 24$) and controls (control 1 ($n = 26$) and control 2 ($n = 21$)). Blue squares show significant positive correlations (0.207 to 0.618, $P < 0.05$), white squares show non-significant correlations ($P > 0.05$), and red squares show significant negative correlations (-0.236 to -0.545, $P < 0.05$). Size of the squares and varying shades of blue and red color show intermediate correlation coefficient values. Endometrial biochemical markers include leukemia inhibitory factor (LIF), E-cadherin, integrin-αv, integrin-β3, mucin 1, MECA79 (L-selectin ligand) and vascular endothelial growth factor (VEGF) and blood flow markers include resistance index (RI), pulsatility index (PI), vascularization index (VI), end diastolic volume (EDV) and S/D (systemic diastolic) ratio.

lactate levels in dormant GTB cases are indicative of anaerobic glycolysis where high lactate limits the source of anaerobic ATP and contributes toward the decline in cellular energy level in TB-infected animal models (Shin *et al.*, 2011; Somashekar *et al.*, 2011). Thus, a significant increase in lactate could be associated with tissue hypoxia and progression of the infection. On the other hand, there is a possibility of the 'Warburg effect' which could enhance glycolysis even in aerobic conditions, as suggested by earlier studies (Zhivotovsky and Orrenius, 2009). An increased level of glycogen and decreased level of glucose in the tubercle-infected endometrium indicates *Mycobacterium tuberculosis* stores glucose as glycogen, an energy storage molecule, in the adverse conditions. Various studies have reported that glycogen plays a crucial role in the pathogenesis of the disease (Bourassa and Camilli, 2009; Gupta *et al.*, 2014).

Elevated levels of Krebs cycle intermediates (citrate, succinate and aspartate) in dormant GTB cases show an increased energy consumption which is consistent with the earlier findings in TB-animal models (Phillis and O'Regan, 1996; Shin *et al.*, 2011; Somashekar *et al.*, 2011). The malate-aspartate shuttle for oxidizing NADH produced by glycolysis becomes non-functional during TB infection (Lane and Gardner, 2005). The increase in tissue aspartate level observed in the present study is possibly due to impairment in the malate-aspartate shuttle of dormant GTB women. It is likely that higher levels of energy metabolites suggest an increase in TCA cycle mediated energy respiration in dormant GTB condition.

Altered lipid and fatty acid metabolism

Using NMR metabolomics, Zhou *et al.* (2013) have reported enhanced lipid degradation in TB patients relative to controls. It is well known that creatine kinase catalyzes the conversion of phosphocreatine to ATP and creatine which supplies energy to the cells in a disease condition due to the increasing energy demand (Wallimann *et al.*, 2011; Chen *et al.*, 2013). Significantly higher creatine levels in women with dormant GTB suggest an increased utilization of the generated ATP and accumulation of creatine in endometrial tissue of these women. Increased levels of succinate and acetate suggest a possible metabolic switch to fatty acid oxidation, thereby increasing the demand for ATP and cell energy supply. These findings indicate that, in the presence of dormant tubercle bacilli, lipids and fatty acids are the possible carbon source for producing energy through β-oxidation under glucose deficiency and oxygen tension (Somashekar *et al.*, 2011; Chen *et al.*, 2013).

Increased choline levels have been associated with cell membrane modification, particularly in tubercular and fungal infections and various inflammatory disorders (Corbin and Zeisel, 2012; St-Coeur *et al.*, 2013). In support of this hypothesis, we found a negative correlation between choline and a number of endometrial receptivity markers (Fig. 3). An increased level of choline in the present study suggests tubercle bacilli mediated dysregulation of host lipid metabolism in the endometrial tissue of women with dormant GTB.

Alterations in amino acid biosynthesis

Various research groups are of the opinion that 'anabolic block' occurs in TB patients associated with malnutrition and wasting (Schwenk and Macallan, 2000; Paton *et al.*, 2004; Zhou *et al.*, 2013). We observed increased levels of amino acids including L-proline, glutamate, L-glutamine, L-valine, L-isoleucine, L-leucine, L-lysine, L-glycine and L-methionine and decreased L-threonine, L-tyrosine, L-phenylalanine in dormant GTB women compared with controls. This may be attributed to a compromised anabolic response owing to infection, where amino acids may be oxidized due to impairment in protein synthesis (Paton *et al.*, 2004; Somashekar *et al.*, 2012; Zhou *et al.*, 2013). A significant increase in amino acids including valine, isoleucine, leucine, and methionine suggests increased Krebs cycle intermediates (aspartate and succinate) to supply energy. These results are in accordance with a report on NMR-based metabolomics of TB patients by Zhou *et al.* (2013).

The regulatory role of lysine in the pathogenesis of TB is well recognized (Kim *et al.*, 2006; Nambi *et al.*, 2013). A recent study by Liu *et al.*

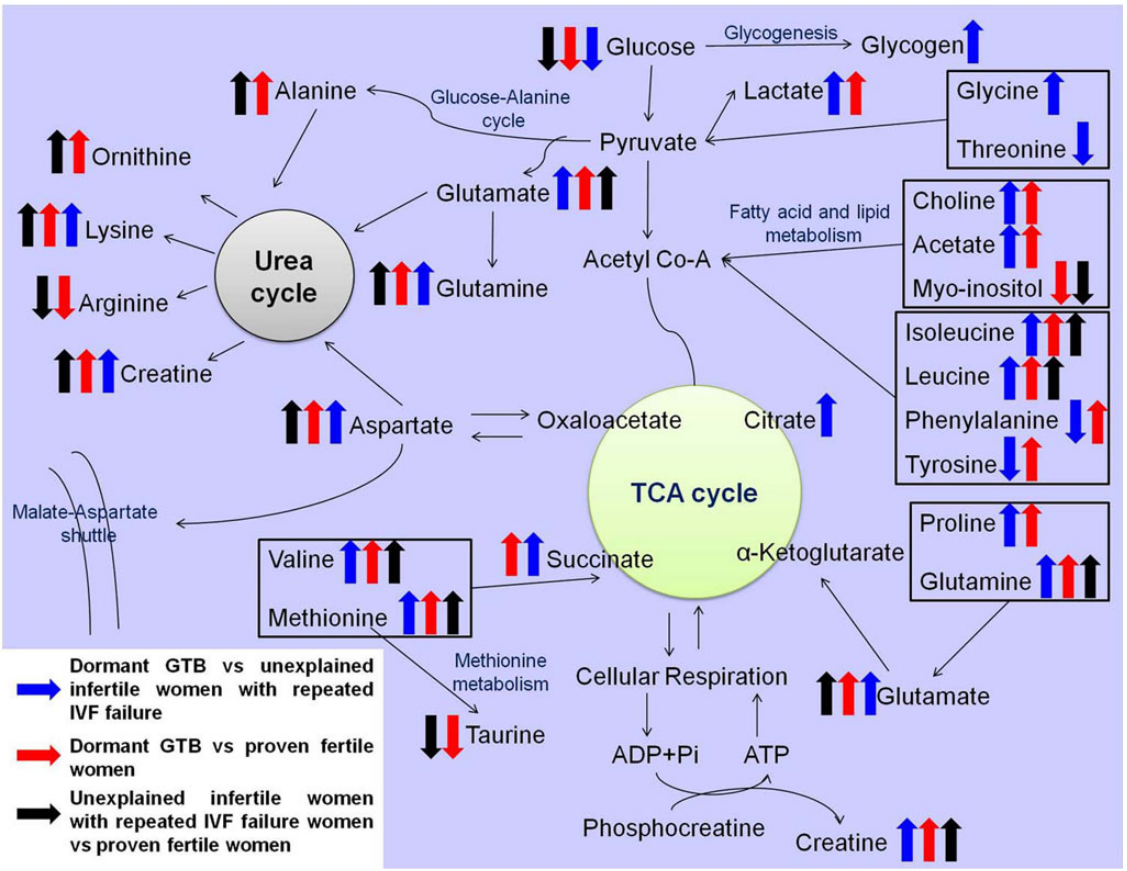

Figure 4 Schematic representation of the altered metabolic pathways in women with dormant GTB and unexplained infertile cases. Overview of altered metabolites in endometrial tissue from dormant GTB cases versus control 1 (red arrows), dormant GTB cases versus control 2 (blue arrows) and control 1 versus control 2 (black arrows). Up-regulation: upward arrows; down-regulation: downward arrows. TCA: tricarboxylic acid.

(2014) reveals the role of lysine acetylation in the metabolic network of *Mycobacterium tuberculosis*. We found L-lysine to be increased in endometrial tissue of women with dormant GTB. It is reported that L-proline plays an important role in pathogenesis and the host-immune response (Smith, 2003; Bhat *et al.*, 2012). Also, L-glutamine and L-glutamate are associated with immunomodulatory activity and inflammation (Banerjee *et al.*, 2014). However, association between these metabolites and an inflammatory response in women with dormant GTB warrants further investigation.

Metabolic changes in the endometrium of unexplained infertile women with repeated implantation failure

On comparing endometrial tissue metabolites of unexplained infertile women and proven fertile controls, we observed 17 metabolites that were significantly dysregulated (Table II). These metabolites are mostly associated with taurine and hypotaurine metabolism, pyruvate metabolism, arginine and proline metabolism, with corresponding changes in protein biosynthesis (Fig. 4; Supplementary Fig. S3B).

Myoinositol is an end-product of lipid metabolism and gets converted to acetyl-CoA for the energy supply. A down-regulation of myoinositol in the cases of unexplained fertility is suggestive of alterations in the lipid metabolism. Our findings are supported by the work of Labarta *et al.* (2011) where functional genomic analysis during the WOI indicates that the myoinositol gene is up-regulated in the normal cycle and down-regulated in women with poor implantation. Also, a study by Unfer *et al.* (2011) has shown that myoinositol supplementation restores the ovarian activity and improves pregnancy outcome. As mentioned above, a high level of creatine in unexplained infertile cases indicates an increased energy demand.

Taurine, a β-amino acid, is found abundantly in various mammalian tissues and in oviductal and uterine fluid (Devreker *et al.*, 1999). The concentration of taurine is higher in human uterine fluid during mid-cycle and the luteal phase owing to endometrial secretions (Casslén, 1987). Taurine plays an important role in osmotic regulation and maintains the motility of spermatozoa in uterine fluid, thereby helping in improving IVF success (Leese *et al.*, 1979; Casslén, 1987). The decreased level of taurine in unexplained cases indicates an unfavorable endometrial environment for implantation. Moreover, since taurine is an end-product of methionine metabolism (Huxtable, 1992; Shi *et al.*, 2012), increased methionine and decreased taurine levels reflect the possibility of alterations in methionine metabolism. The observed findings suggest changes in cellular energy metabolism in women with unexplained infertility.

A significant increase in amino acids including L-valine, L-leucine, L-isoleucine, L-glutamate, L-glutamine, L-lysine, L-alanine, L-tyrosine, L-phenylalanine and methionine was observed in unexplained infertile women compared with controls. This signifies protein biosynthesis alterations in these cases. A role of L-arginine in the reproductive performance of rats (Zeng *et al.*, 2008) and mice (Greene *et al.*, 2012) has been demonstrated. The increased number of implantation sites in mice with L-arginine supplementation explains how L-arginine supports the endometrium to be receptive (Greene *et al.*, 2012). Moreover, higher concentration of L-arginine in human uterine flushes during the proliferative phase suggests its involvement in the proliferation of endometrial cells and providing a suitable environment for embryo-endometrial interaction (Casslen, 1987; Greene *et al.*, 2013; Zhang *et al.*, 2013). A significant decrease in L-arginine of unexplained infertile women suggests a poor receptive state of the endometrium. Increased levels of ornithine in dormant GTB cases indicate the conversion of L-arginine into ornithine by arginase, which is an enzymatic process of polyamine synthesis (Greene *et al.*, 2013). Hence, it is reasonable to presume that an increased conversion of arginine to ornithine and urea depletes the levels of arginine available for nitric oxide synthesis: this is reflected by the altered arginine-ornithine ratio in unexplained cases. Moreover, the simultaneous increase in lysine and decrease in arginine reflect the increased uptake of arginine in these cases, since L-arginine and L-lysine share the same intracellular transporter system. A decrease in glucose and simultaneous increase in alanine show the involvement of the glucose-alanine pathway in unexplained infertile cases. Under anaerobic cellular respiration, energy is produced via glucose-alanine cycle as an alternate energy metabolism (Ho *et al.*, 2014).

Conclusions

With the combined use of 1H NMR spectroscopy and multivariate analysis, we have successfully identified the major metabolites contributing toward discrimination between women with dormant GTB and controls. Significant alterations in metabolites, largely related to energy metabolism with corresponding changes in intermediates of lipid metabolism, amino acid biosynthesis and reduction of sugars, in dormant GTB cases underline the metabolic influence associated with the tubercle infection, even in its inactive form (Fig. 4). Though the cause-and-effect relationship remains unclear/unproven, we found the metabolic changes in the endometrium of women with dormant GTB during the WOI to be associated with the poor endometrial status of these women. One of the limitations of this study is that we did not test prostate-specific antigen or Y chromosome in these women, which could have provided important information related to the possible influence of recent semen exposure on the endometrium of women with GTB.

Supplementary data

Supplementary data are available at http://humrep.oxfordjournals.org/.

Acknowledgements

The authors are grateful to all the volunteers who participated in this study. One of the authors, E.S., is thankful to IIT Kharagpur and MHRD, Govt. of India for fellowship.

Authors' roles

E.S. was involved in study design, assaying samples, data analysis and interpretation and manuscript drafting. M.J. performed the data analysis, interpretation and manuscript drafting. M.D. and D.C. were contributed to study design, manuscript drafting and critical discussion. M.J. and S.S. performed NMR instrumentation and helped in data analysis. A.M. was contributed in data analysis and interpretation. C.D.R. and B.N.C. conceived the study and provided clinical inputs. B.N.C. has also performed uterine curettage (D&C). K.C. was involved in study design, data interpretation, manuscript drafting and critical discussion; all authors revised the manuscript and approved the final version.

Funding

This study was funded by Government of India, Indian Council of Medical Research.

Conflict of interest

None declared.

References

Banerjee P, Jana SK, Pasricha P, Ghosh S, Chakravarty B, Chaudhury K. Proinflammatory cytokines induced altered expression of cyclooxygenase-2 gene results in unreceptive endometrium in women with idiopathic recurrent spontaneous miscarriage. *Fertil Steril* 2013;**99**:179–187.

Banerjee P, Dutta M, Srivastava S, Joshi M, Chakravarty B, Chaudhury K. (1)H NMR serum metabonomics for understanding metabolic dysregulation in women with idiopathic recurrent spontaneous miscarriage during implantation window. *J Proteome Res* 2014;**13**:3100–3106.

Beckonert O, Keun HC, Ebbels TM, Bundy J, Holmes E, Lindon JC, Nicholson JK. Metabolic profiling, metabolomic and metabonomic procedures for NMR spectroscopy of urine, plasma, serum and tissue extracts. *Nat Protoc* 2007;**2**:2692–2703.

Bhat KH, Chaitanya CK, Parveen N, Varman R, Ghosh S, Mukhopadhyay S. Proline-proline-glutamic acid (PPE) protein Rv1168c of Mycobacterium tuberculosis augments transcription from HIV-1 long terminal repeat promoter. *J Biol Chem* 2012;**287**:16930–16946.

Bourassa L, Camilli A. Glycogen contributes to the environmental persistence and transmission of Vibrio cholera. *Mol Microbiol* 2009;**72**:124–138.

Bujak R, Garcia-Alvarez A, Ruperez FJ, Nuno-Ayala M, Garcia A, Ruiz-Cabello J, Fuster V, Ibanez B, Barbas C. Metabolomics reveals metabolite changes in acute pulmonary embolism. *J Proteome Res* 2014;**13**:805–816.

Casslen BG. Free amino acids in human uterine fluid. Possible role of high taurine concentration. *J Reprod Med* 1987;**32**:181–184.

Chen Y, Wu J, Tu L, Xiong X, Hu X, Huang J, Xu Z, Zhang X, Hu C, Hu X *et al.* (1)H-NMR spectroscopy revealed Mycobacterium tuberculosis caused abnormal serum metabolic profile of cattle. *PLoS One* 2013;**8**:e74507.

Corbin KD, Zeisel SH. Choline metabolism provides novel insights into nonalcoholic fatty liver disease and its progression. *Curr Opin Gastroenterol* 2012;**28**:159–165.

Dam P, Shirazee HH, Goswami SK, Ghosh S, Ganesh A, Chaudhury K, Chakravarty B. Role of latent genital tuberculosis in repeated IVF failure in the Indian clinical setting. *Gynecol Obstet Invest* 2006;**61**:223–227.

Das P, Ahuja A, Gupta SD. Incidence, etiopathogenesis and pathological aspects of genitourinary tuberculosis in India: a journey revisited. *Indian J Urol* 2008;**24**:356–361.

Devreker F, Van den Bergh M, Biramane J, Winston RL, Englert Y, Hardy K. Effects of taurine on human embryo development in vitro. *Hum Reprod* 1999;**14**:2350–2356.

Dutta M, Joshi M, Srivastava S, Lodh I, Chakravarty B, Chaudhury K. A metabonomics approach as a means for identification of potential biomarkers for early diagnosis of endometriosis. *Mol Biosyst* 2012;**8**:3281–3287.

Frediani JK, Jones DP, Tukvadze N, Uppal K, Sanikidze E, Kipiani M, Tran VT, Hebbar G, Walker DI, Kempker RR *et al.* Plasma metabolomics in human pulmonary tuberculosis disease: a pilot study. *PLoS One* 2014; **9**:e108854.

Galliano D, Bellver J, Diaz-Garcia C, Simon C, Pellicer A. ART and uterine pathology: how relevant is the maternal side for implantation? *Hum Reprod Update* 2015;**21**:13–38.

Gatongi DK, Gitau G, Kay V, Ngwenya S, Lafong C, Hasan A. Female genital tuberculosis. *Obstet Gynaecol* 2005;**7**:75–79.

Ghosh S, Chattopadhyay R, Goswami S, Ganesh A, Chaudhury K, Chakravarty B. Recurrent implantation success in consecutive embryo transfer cycles: a unique case report. *Syst Biol Reprod Med* 2013;**59**:285–286.

Greene JM, Dunaway CW, Bowers SD, Rude BJ, Feugang JM, Ryan PL. Dietary L-arginine supplementation during gestation in mice enhances reproductive performance and Vegfr2 transcription activity in the fetoplacental unit. *J Nutr* 2012;**142**:456–460.

Greene JM, Feugang JM, Pfeiffer KE, Stokes JV, Bowers SD, Ryan PL. L-Arginine enhances cell proliferation and reduces apoptosis in human endometrial RL95-2 cells. *Reprod Biol Endocrinol* 2013;**11**:15.

Gupta AK, Singh A, Singh S. Glycogenomics of Mycobacterium tuberculosis. *Mycobact Dis* 2014;**4**:6.

Haouzi D, Mahmoud K, Fourar M, Bendhaou K, Dechaud H, De Vos J, Reme T, Dewailly D, Hamamah S. Identification of new biomarkers of human endometrial receptivity in the natural cycle. *Hum Reprod* 2009; **24**:198–205.

Hedjazi L, Gauguier D, Zalloua PA, Nicholson JK, Dumas ME, Cazier JB. mQTL.NMR: an integrated suite for genetic mapping of quantitative variations of (1)H NMR-based metabolic profiles. *Anal Chem* 2015; **87**:4377–4384.

Ho WE, Xu YJ, Cheng C, Peh HY, Tannenbaum SR, Wong WS, Ong CN. Metabolomics reveals inflammatory-linked pulmonary metabolic alterations in a murine model of house dust mite-induced allergic asthma. *J Proteome Res* 2014;**13**:3771–3782.

Huxtable RJ. Physiological actions of taurine. *Physiol Rev* 1992;**72**:101–163.

Jana SK, Dutta M, Joshi M, Srivastava S, Chakravarty B, Chaudhury K. 1H NMR based targeted metabolite profiling for understanding the complex relationship connecting oxidative stress with endometriosis. *Biomed Res Int* 2013;**2013**:329058.

Kim SC, Sprung R, Chen Y, Xu Y, Ball H, Pei J, Cheng T, Kho Y, Xiao H, Xiao L *et al.* Substrate and functional diversity of lysine acetylation revealed by a proteomics survey. *Mol Cell* 2006;**23**:607–618.

Kocher C, Weber R, Friedl A. A case study of female genital tuberculosis in a Western European setting. *Infection* 2011;**39**:59–63.

Kostara CE, Papathanasiou A, Psychogios N, Cung MT, Elisaf MS, Goudevenos J, Bairaktari ET. NMR-based lipidomic analysis of blood lipoproteins differentiates the progression of coronary heart disease. *J Proteome Res* 2014;**13**:2585–2598.

Labarta E, Martínez-Conejero JA, Alamá P, Horcajadas JA, Pellicer A, Simón C, Bosch E. Endometrial receptivity is affected in women with high circulating progesterone levels at the end of the follicular phase: a functional genomics analysis. *Hum Reprod* 2011;**26**:1813–1825.

Lane M, Gardner DK. Mitochondrial malate-aspartate shuttle regulates mouse embryo nutrient consumption. *J Biol Chem* 2005;**280**:18361–18367.

Leese HJ, Aldridge S, Jeffries KS. The movement of amino acids into rabbit oviductal fluid. *J Reprod Fertil* 1979;**56**:623–626.

Liu F, Yang M, Wang X, Yang S, Gu J, Zhou J, Zhang XE, Deng J, Ge F. Acetylome analysis reveals diverse functions of lysine acetylation in Mycobacterium tuberculosis. *Mol Cell Proteomics* 2014;**13**:3352–3366.

Malik S. Genital tuberculosis and implantation in assisted reproduction. *Rev Gynaecol Pract* 2003;**3**:160–164.

Margalioth EJ, Ben-Chetrit A, Gal M, Eldar-Geva T. Investigation and treatment of repeated implantation failure following IVF-ET. *Hum Reprod* 2006;**21**:3036–3043.

Martin J, Dominguez F, Avila S, Castrillo JL, Remohi J, Pellicer A, Simon C. Human endometrial receptivity: gene regulation. *J Reprod Immunol* 2002; **55**:131–139.

Mazzei P, Piccolo A, Nugnes L, Mascolo M, De Rosa G, Staibano S. Metabolic profile of intact tissue from uterine leiomyomas using high-resolution magic-angle-spinning ^{1}H NMR spectroscopy. *NMR Biomed* 2010; **23**:1137–1145.

Nambi S, Gupta K, Bhattacharyya M, Ramakrishnan P, Ravikumar V, Siddiqui N, Thomas AT, Visweswariah SS. Cyclic AMP-dependent protein lysine acylation in mycobacteria regulates fatty acid and propionate metabolism. *J Biol Chem* 2013;**288**:14114–14124.

Paton NI, Chua YK, Earnest A, Chee CB. Randomized controlled trial of nutritional supplementation in patients with newly diagnosed tuberculosis and wasting. *Am J Clin Nutr* 2004;**80**:460–465.

Phillis JW, O'Regan MH. Mechanisms of glutamate and aspartate release in the ischemic rat cerebral cortex. *Brain Res* 1996;**730**:150–164.

Rozati R, Roopa S, Rajeshwari CN. Evaluation of women with infertility and genital tuberculosis. *J Obstet Gynecol India* 2006;**56**:423–426.

Sankar MM, Kumar P, Munawwar A, Kumar M, Singh J, Singh A, Parashar D, Malhotra N, Duttagupta S, Singh S. Usefulness of multiplex PCR in the diagnosis of genital tuberculosis in females with infertility. *Eur J Clin Microbiol Infect Dis* 2013;**32**:399–405.

Schwenk A, Macallan DC. Tuberculosis, malnutrition and wasting. *Curr Opin Clin Nutr Metab Care* 2000;**3**:285–291.

Shi X, Yao D, Chen C. Identification of N-acetyltaurine as a novel metabolite of ethanol through metabolomics-guided biochemical analysis. *J Biol Chem* 2012;**287**:6336–6349.

Shin JH, Yang JY, Jeon BY, Yoon YJ, Cho SN, Kang YH, Ryu do H, Hwang GS. (1)H NMR-based metabolomic profiling in mice infected with mycobacterium tuberculosis. *J Proteome Res* 2011;**10**:2238–2247.

Smith I. Mycobacterium tuberculosis pathogenesis and molecular determinants of virulence. *Clin Microbiol Rev* 2003;**16**:463–496.

Somashekar BS, Amin AG, Rithner CD, Troudt J, Basaraba R, Izzo A, Crick DC, Chatterjee D. Metabolic profiling of lung granuloma in *Mycobacterium tuberculosis* infected guinea pigs: ex vivo 1H magic angle spinning NMR studies. *J Proteome Res* 2011;**10**:4186–4195.

Somashekar BS, Amin AG, Tripathi P, MacKinnon N, Rithner CD, Shanley CA, Basaraba R, Henao-Tamayo M, Kato-Maeda M, Ramamoorthy A *et al.* Metabolomic signatures in guinea pigs infected with epidemic-associated W-Beijing strains of Mycobacterium tuberculosis. *J Proteome Res* 2012; **11**:4873–4884.

St-Coeur PD, Touaibia M, Cuperlovic-Culf M, Morin P Jr. Leveraging metabolomics to assess the next generation of temozolomide-based therapeutic approaches for glioblastomas. *Genomics Proteomics Bioinformatics* 2013;**11**:199–206.

Subramani E, Madogwe E, Bordignon V, Duggavathi R, Ray CD, Dutta SK, Chakravarty BN, Chaudhury K. Dysregulated LIF and its receptor regulated STAT3 pathway: a possible cause for repeated implantation failure in women with dormant genital tuberculosis? *Fertil Steril* 2016 (in press).

Thangappah RBP, Paramasivan CN, Narayanan S. Evaluating PCR, culture & histopathology in the diagnosis of female genital tuberculosis. *Indian J Med Res* 2011;**134**:40–46.

Unfer V, Raffone E, Rizzo P, Buffo S. Effect of a supplementation with myoinositol plus melatonin on oocyte quality in women who failed to conceive in previous in vitro fertilization cycles for poor oocyte quality: a prospective, longitudinal, cohort study. *Gynecol Endocrinol* 2011;**27**:857–861.

Wallimann T, Tokarska-Schlattner M, Schlattner U. The creatine kinase system and pleiotropic effects of creatine. *Amino Acids* 2011;**40**:1271–1296.

Weiner J III, Parida SK, Maertzdorf J, Black GF, Repsilber D, Telaar A, Mohney RP, Arndt-Sullivan C, Ganoza CA, Fae KC *et al.* Biomarkers of inflammation, immunosuppression and stress with active disease are revealed by metabolomic profiling of tuberculosis patients. *PLoS One* 2012;**7**:e40221.

Wilcox AJ, Baird DD, Weinberg CR. Time of implantation of the conceptus and loss of pregnancy. *N Engl J Med* 1999;**340**:1796–1799.

Xia J, Wishart DS. MetPA: a web-based metabolomics tool for pathway analysis and visualization. *Bioinformatics* 2010;**26**:2342–2344.

Zeng X, Wang F, Fan X, Yang W, Zhou B, Li P, Yin Y, Wu G, Wang J. Dietary arginine supplementation during early pregnancy enhances embryonic survival in rats. *J Nutr* 2008;**138**:1421–1425.

Zhang S, Lin H, Kong S, Wang S, Wang H, Wang H, Armant DR. Physiological and molecular determinants of embryo implantation. *Mol Aspects Med* 2013;**34**:939–980.

Zhao X, Chen J, Ye L, Xu G. Serum metabolomics study of the acute graft rejection in human renal transplantation based on liquid chromatography-mass spectrometry. *J Proteome Res* 2014;**13**:2659–2667.

Zhivotovsky B, Orrenius S. The Warburg Effect returns to the cancer stage. *Semin Cancer Biol* 2009;**19**:1–3.

Zhou A, Ni J, Xu Z, Wang Y, Lu S, Sha W, Karakousis PC, Yao YF. Application of (1)H NMR spectroscopy-based metabolomics to sera of tuberculosis patients. *J Proteome Res* 2013;**12**:4642–4649.